

# PAL\*M: Property Attestation for Large Generative Models

Prach Chantasantitam<sup>1</sup>, Adam Ilyas Caulfield<sup>1</sup>, Vasisht Duddu<sup>1</sup>, Lachlan J. Gunn<sup>2</sup>, N. Asokan<sup>1,3</sup>

<sup>1</sup>*University of Waterloo*, <sup>2</sup>*Aalto University*, <sup>3</sup>*KTH Royal Institute of Technology*

*{pchantas, acaulfield, vasisht.duddu}@uwaterloo.ca, lachlan@gunn.ee, asokan@acm.org}*

## Abstract

*Machine learning property attestations* allow provers (e.g., model providers or owners) to attest properties of their models/datasets to verifiers (e.g., regulators, customers), enabling accountability towards regulations and policies. But, current approaches do not support generative models or large datasets. We present PAL\*M, a property attestation framework for large generative models, illustrated using large language models. PAL\*M defines properties across training and inference, leverages *confidential virtual machines* with *security-aware* GPUs for coverage of CPU-GPU operations, and proposes using *incremental multiset hashing* over memory-mapped datasets to efficiently track their integrity. We implement PAL\*M on Intel TDX and NVIDIA H100, showing it is efficient, scalable, versatile, and secure.

## 1 Introduction

Machine learning (ML) models are widely deployed across domains such as healthcare, finance, and autonomous systems [30, 69, 71]. Emerging regulations (e.g., EU’s AI Act [3]) require models meet certain *properties* related to accuracy, training procedures, data provenance, and inference. Providing proof of such properties may be challenging for confidential datasets or models.

*ML property attestation* enables a *model provider* (Prv) to demonstrate properties about their model or datasets to a *verifier* (Vrf) [16]. Approaches based on *trusted execution environments* (TEEs) [5, 7, 36, 37], first proposed in Laminator [17], has been shown to be efficient, scalable, versatile, and secure for classifiers, whereas alternative approaches based on zero-knowledge proofs [1, 23, 31, 41, 56, 63] or re-purposing of inference attacks [18, 72] do not meet all requirements.

But, Laminator does not scale to generative models, such as large language models (LLMs). For example, large datasets cannot reside fully in TEE memory and are accessed via *random sampling* from untrusted storage, undermining standard integrity measurement strategies.

Enabling ML property attestations for generative models requires addressing three challenges: (1) handling of large datasets outside of TEE memory sampled in a *random* fashion, (2) supporting CPU-GPU computing environments, and (3) defining property attestation for common operations related to generative models. We address these challenges with PAL\*M, the first framework for *ML property attestations of large generative models*, using LLMs for illustration.

PAL\*M employs *incremental multiset hashing* [14] to enable compact secure integrity tracking of large, randomly-accessed, datasets, and TEE-aware GPUs to efficiently and securely ensure integrity of heterogeneous operations. Finally, we define property attestations for a comprehensive set of operations (e.g., fine-tuning, quantization, LLM chat sessions) that do not require revealing confidential datasets or models to Vrf. We prototype and evaluate PAL\*M using Intel TDX and NVIDIA H100.

In summary, we claim the following contributions: we

1. use incremental multiset hash functions to construct representative measurements of datasets in external storage that are randomly sampled at run-time (Section 4.2);
2. define how to measure properties of generative model operations, incorporating GPU attestation evidence without exposing confidential details (Section 4.3);
3. specify a property attestation protocol that shows how such measurements and outputs can be combined to prove data/models were produced by a PAL\*M-equipped CPU-GPU configuration (Section 4.4); and
4. implement and evaluate PAL\*M on Intel TDX and NVIDIA H100 with real-world datasets/models, showing it meets all requirements (Sections 5 and 6).

## 2 Background

### 2.1 Large Language Models

**Training.** LLMs use transformer architectures with billions of parameters [11, 70], and are trained to predict the next tokens given previous ones. During training, the model learns a

probability distribution of the next token from a vocabulary to follow a sequence of tokens. This is often called *pretraining*, as it is typically followed by another phase of training for task-specific optimization/tuning.

**Tokenizers.** Modern tokenizers operate at word, sub-word (e.g., byte pair encoding, WordPiece), or character level to convert natural-language text into numerical representations for use during LLM training and inference.

**Fine-tuning.** Since training LLMs is resource- and time-intensive, publicly available trained LLMs are generally fine-tuned on a task-specific dataset. Parameter-Efficient Fine-Tuning (PEFT) and Low-Rank Adaptation (LoRA) fine-tune a small subset of model parameters instead of retraining the entire model [29, 44]. Alternatively, *adapter layers* are trainable modules that can be attached to a pretrained LLM, enabling task-specific adaptation without altering the core model parameters. These approaches are more efficient than fine-tuning the entire LLM.

**Evaluating LLMs.** Benchmarks for LLMs cover a variety of tasks and compute relevant metrics. These tasks span language understanding (e.g., MMLU [27]), math problems, multiple-choice, classification, and open-ended question answering. Each category is designed to probe specific capabilities of the model across common benchmarks.

**Chat sessions.** LLMs are commonly used for chatbots, which allow a user to continuously query about a particular task and get the responses from the model that consider prior conversational context (e.g., OpenAI’s ChatGPT). Chat sessions contain multiple user queries and their responses.

**Memory Management.** Large generative models require significantly more data than traditional ML models, which often do not fit into main memory (e.g., Pile dataset is over 800 GB [21]). Instead of loading the entire data into memory, current LLM libraries (e.g., Hugging Face) support *memory-mapped datasets* [32], which map the contents of a file into a process’s virtual memory space, allowing it to be accessed like regular memory, rather than through explicit file I/O operations, despite residing on disk. When a dataset is memory-mapped, dataset records are only loaded into memory as needed, significantly reducing memory usage.

**Data Transformations and Processing:** Before a dataset is used, it typically undergoes a series of transformations, including *preprocessing* steps like normalization, concatenation, truncation, tokenization, and splitting into training, validation, and test sets, as well as additional processing for removing corrupted samples and formatting the data to match the expected input structure of the training framework [33].

During training, *random sampling* is commonly used to reduce bias introduced by data ordering and to improve model generalization [55]. PyTorch’s DataLoader and Sampler abstractions provide randomized sampling [51]. Popular training libraries, such as Hugging Face Transformers, support random sampling and enable it for default training pipelines [34].

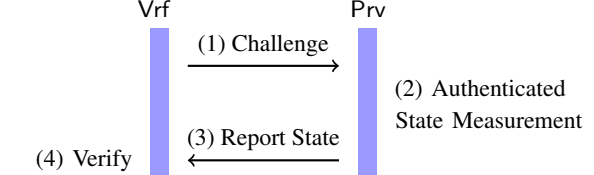


Figure 1: Traditional remote attestation protocol: a prover (Prv) demonstrates its software integrity to a verifier (Vrf).

## 2.2 Trusted Execution Environments

TEEs are a set of architectural components that provide a secure execution environment that is isolated from the “rich” host environment. They guarantee that software executing outside of the TEE cannot directly read or write to data inside the TEE’s trusted boundary. The exact details of the trusted boundary vary based on the particular approach. For example, Intel SGX [36] creates TEE in the user-space *enclaves* and ARM TrustZone [7] creates a TEE containing all system resources (e.g., separate trusted OS and applications with dedicated peripherals).

Recent technologies have also introduced *confidential virtual machines* (CVMs), which enable entire VMs to execute within the trust boundary of a TEE (e.g., AMD SEV-SNP [5], Intel TDX [37], and ARM Realms [40]). An advantage provided by CVMs is that they enable executing unmodified and full-feature operating systems without requiring TEE-specific rewrites. Additionally, TEE-aware GPUs have recently emerged (e.g., with NVIDIA H100 GPU). As such, CVM providers have released drivers to support integration with TEE-aware GPUs. This has enabled the potential for heavy computations (e.g., ML training) within a TEE. Both CPUs and GPUs with TEEs typically support *remote attestation* to prove trustworthiness to verifiers.

Intel Trust Domain eXtensions (TDX) [37] enables isolated CVMs in the form of trust domains (TDs). Upon creation of a TD, invoked by the untrusted virtual machine manager (VMM), the TDX module computes a measurement of TD components during TD creation, which can be used later for attestation. To attest TD’s state, the TD invokes the TDX module to generate a TDREPORT, which is generated by the CPU computing a MAC over measurements of the TD image, the TDX module image, and any REPORTDATA extended by the TD at runtime. The resulting TDREPORT and MAC are passed by the TDX Module to the quoting enclave (QE), a special-purpose Intel SGX enclave [38]. The QE uses contents of TDREPORT to generate a SGX-style QUOTE using a provisioning certification key [35]. Before generating this QUOTE, the QE first validates the MAC, ensuring integrity is maintained when passed by the untrusted VMM.

## 2.3 Attestation Protocols

Remote attestation is a protocol in which a verifier (Vrf) challenges a prover (Prv) to demonstrate that they are installed with the correct configurations [46]. The steps for a traditional remote attestation protocol are visualized in Figure 1. The authenticated integrity measurement in step (2) is computed by Prv's *root of trust* (RoT) and is typically a message authenticated code (MAC) or digital signature. Thus, one requirement of remote attestation is that Prv's RoT can securely store and use a private key, implying some level of hardware assistance. Hence, TEEs can naturally enable remote attestation with their properties for isolated data and execution. For Intel TDX, step (2) involves computing TDREPORT and QUOTE.

Property attestation [57] is where Vrf is interested in *properties* of Prv's configuration rather than a specific configuration itself. Here, Vrf obtains the authenticated integrity measurement from Prv, while also obtaining reference values that correspond to a particular property from a *trusted authority* (Tru). If the state measurement from Prv is among the reference values obtained from Tru, and was signed using the expected public key from Prv, Vrf trusts that the property holds on Prv. Notably, unlike standard remote attestation, property attestation requires Vrf to obtain reference values from Tru rather than to recompute them. Every property of interest is associated with a *measurer* on Prv used to measure the state of the property.

The notion of property attestation has been extended recently to cover ML data and processes [16, 17, 57]. In particular, Laminator [17] leverages Intel SGX [36] to attest properties of training data, model, and training process. This works by executing ML operations inside an SGX enclave, measuring the inputs and outputs of the target operation (e.g., training, inference, or dataset statistics), and using SGX’s quote mechanism to return these measurements to the verifier that issued the attestation challenge. Such attestations can then be used for verifiable ML property cards for transparency (e.g., model card, datasheet, and inference card).

### 3 Problem Statement

Our goal is to design a property attestation framework for generative models to prove to Vrf that a claimed property is (a) correctly measured and (b) not false or manipulated.

Unlike typical remote attestation, which is an interactive protocol between Vrf and Prv, ML property attestation must be non-interactive with Vrf. We propose the protocol depicted in Figure 2. Prv interacts with an *initiator* (Inr), who sends a request to Prv for a particular operation, along with other request-specific data (e.g., inputs or a challenge when freshness is required). Upon request, Inr makes them available for Vrf, who may consult Tru for property reference values to verify the evidence.

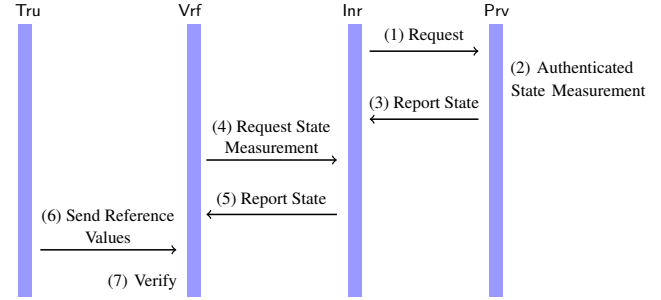


Figure 2: Desired property attestation for ML, in which  $\text{Prv}$  interacts with an Initiator ( $\text{Inr}$ ).  $\text{Vrf}$  requests evidence from  $\text{Inr}$ , and may consult a Trusted Authority ( $\text{Tru}$ ) to obtain reference values of a desired property.

### 3.1 System Model

We consider  $\text{Prv}$  that trains, evaluates, or deploys a model  $\mathcal{M}$ . We consider software that is already executing within CVMs, as ML companies today are exploring use of CVMs [6, 10, 50], and major cloud service providers (e.g., Amazon AWS, Google Cloud, and Microsoft Azure) support TEE-aware GPUs. We consider Intel TDX and NVIDIA H100 in this work, but our framework can be extended to any CVM or TEE-aware GPU (see Section 8).

Property attestations have the following components:

- ***Operation (op)***: a computational task over inputs ( $I$ ) to produce outputs ( $O$ );
- ***Property***: an expression that describes semantics of some meaningful relationship between  $op$ ,  $I$ , and  $O$ ;
- ***Attestation evidence***: a verifiable claim that aims to prove whether a property holds true;

We assume an attestation mechanism on  $\text{Prv}$  executes  $op$  and produces attestation evidence. Obtaining attestation evidence requires (1) measuring  $op$ ,  $I$ ,  $O$  and (2) reporting those measurements by producing a cryptographic token (e.g., a digital signature) binding them. For the latter, a signing key is used that must be only accessible to the attestation mechanism.

### 3.2 Adversary Model

We assume an adversary ( $\mathcal{A}$ dv), in line with the common Intel TDX adversary model [4], who has control over the host machine and the VMM. As a consequence,  $\mathcal{A}$ dv can access and manipulate any memory or device that is not within the trusted boundaries (e.g., other VMs, disk, I/O peripherals). The TDX module and TDX-aware CPU are trusted to be implemented correctly and provide their described functionality for inter-TD memory isolation, isolation from host VMM, and hardware-protected measurement and reporting (e.g., via a QUOTE) of TD images. Since TD creation is managed by  $\mathcal{A}$ dv-controlled VMM, TDs are not inherently trusted. Hence, TDX supports attestation via QUOTE (see Section 2).

We assume NVIDIA H100 GPU hardware is trusted, which measures and attests to its configuration (e.g., boot ROM,

firmware, in confidential computing mode). By default, the interface between a GPU and the TD is not trusted; the GPU and all its memory are brought under the TD’s protection only when the GPU is directly assigned by the VMM [38]. This includes mapping its communication buffers into TD shared memory. TD must obtain an attestation token from the GPU to determine that the assigned device has the anticipated configuration.

At run-time,  $\mathcal{A}dv$  may attempt to obtain confidential data or interfere with the execution of  $op$  in a TD.  $\mathcal{A}dv$  also may attempt to forge QUOTES, either by learning the signing key or by tampering with relevant code/data without detection. We assume a Dolev-Yao  $\mathcal{A}dv$  as it relates to the network (i.e.,  $\mathcal{A}dv$  carries the message). Therefore,  $\mathcal{A}dv$  may attempt to inject or modify messages sent/received by  $Prv$ . However, we consider denial-of-service attacks out of scope. Side channels can be exploited to leak keys. To mitigate these attacks, additional mechanisms (e.g., constant-time software) should be added. However, this is an orthogonal research direction. We consider physical attacks on hardware as out of scope.

### 3.3 Challenges and Requirements

Prior works [17, 24, 53, 59, 62] demonstrate methods to attest ML models using TEEs, but require operations to stay within the one TEE. For example, Laminator [17] requires that all computations stay inside an SGX enclave to ensure integrity. However, this is not possible with reasonable performance of LLM operations. For example, large datasets may require datasets to reside in external storage during operation and require accelerators (e.g., GPUs or NPUs) for reasonable performance (recall Section 2). Although it is possible to outsource computations from a TEE to a standard GPU [39, 68], this adds significant overhead and would not preserve integrity of property measurements without additional measures. Furthermore, no prior work defines *properties* of generative models (e.g., from operations like fine-tuning, quantization, and chat sessions). Therefore, it is unclear how to perform property attestation in a way that is relevant for  $Vrf$  while protecting confidential assets of  $Prv$ .

Due to these challenges, prior work cannot apply to properties of generative models, requiring another approach to address the following concerns:

- (i) accounting for random sampling of large datasets from (untrusted) external storage devices;
- (ii) handling operations that depend on both CPU and GPU with reasonable computational overhead;
- (iii) defining how to measure properties of generative models in a way that is relevant for  $Vrf$  and does not reveal  $Prv$ ’s confidential assets.

Based on these challenges, we consider the following requirements for designing  $PAL^*M$ :

[R1] *Efficient* (low-overhead compared to confidential computing in the same environment),

- [R2] *Scalable* (supports large numbers of provers/verifiers),
- [R3] *Versatile* (supports a variety of properties; requires minimal effort for custom property measurement; can be ported to any CVM/TEE-based GPU configuration), and
- [R4] *Secure* (a malicious  $Prv$  cannot generate attestations of false information).

## 4 $PAL^*M$ Design

### 4.1 Overview of $PAL^*M$

$PAL^*M$  enables  $Prv$  to attest properties of generative models through (1) design of a TD that effectively measures the operation corresponding to a particular property and (2) use of attestation support from Intel TDX and NVIDIA H100 to construct authenticated evidence these measurements. Figure 3 shows a high-level overview of a  $Prv$ ’s workflow with  $PAL^*M$  and the interaction between  $Prv$  and  $Inr$ .

In 1,  $Inr$  requests a property attestation by specifying: (a) the requested operation ( $op$ ), (b) an attestation challenge ( $Chal$ ), and any inputs that should be used (e.g., datasets, models, configuration parameters, inference query). Upon receipt,  $Prv$ ’s VMM saves all data to disk. In 2, inputs are fetched by  $PAL^*M$  into TD memory according to the dataset access strategy (discussed further in Section 4.2). Based on  $op$ , the corresponding function will start to execute in 3. While executing, outputs will be obtained by a combination of CPU execution 4a and GPU execution 4b. Operation outputs and attestation measurements are obtained 5. When a GPU is used, the attestation measurements include a GPU-attestation token ( $GPU_{att}$ ).

After outputs are obtained,  $PAL^*M$  TD leverages TDX mechanisms to convert property attestation measurements into authenticated evidence. As a first step, it invokes the TDX module in 6 to generate an authenticated  $TDREPORT$  containing  $PAL^*M$  attestation measurements. To complete the quote process,  $TDREPORT$  is passed to the VMM in 7, which invokes the QE in 8 to convert  $TDREPORT$  into a QUOTE. Finally, QUOTE is returned to  $Inr$  in 9.  $Inr$  will provide QUOTE and outputs to requesting  $Vrf$ , who consults Tru (e.g., Intel and NVIDIA) to perform evidence verification. Protocol details are described further in Section 4.4.

By design,  $PAL^*M$  generates QUOTES that attest to properties of generative model operations, while addressing key challenges:

1.  $PAL^*M$  leverages *incremental multiset hash functions* [14] to ensure large datasets are accurately reflected in attestation evidence despite residing in untrusted external storage devices and being randomly sampled;
2.  $PAL^*M$  ensures measurements of both CPU and GPU configurations are captured in attestation evidence for properties that depend on CPU and GPU;

Building upon these capabilities, we show how to define, measure, and attest to properties of the following generative

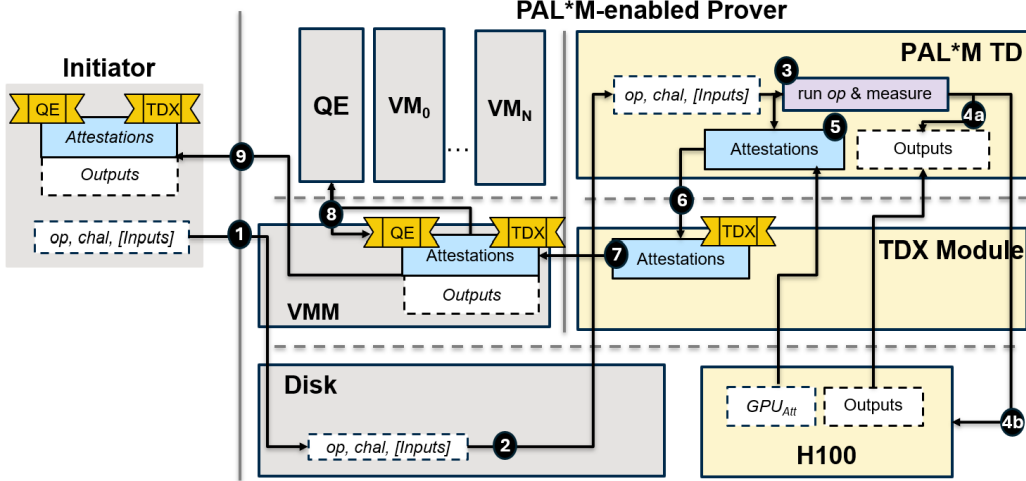


Figure 3: High-level overview of PAL\*M-enabled property attestation.  $\text{Inr}$  interacts with untrusted components of  $\text{Prv}$ , which saves inputs to disk. PAL\*M reads and measures inputs, runs the operations (including GPU), and measures all CPU and GPU outputs. All measurements are extended to  $\text{REPORTDATA}$ , which is used to as input to obtain  $\text{TDREPORT}$  from TDX Module. Finally, a QUOTE is generated by invoking the Quoting Enclave (QE) and returned to  $\text{Inr}$ .

model operations (from Section 2.1):

1. dataset transformations and distributional statistics;
2. model pretraining, optimization (e.g., fine-tuning, quantization), and evaluation;
3. model interactions (e.g., inference or chat sessions).

## 4.2 Dealing with Large Datasets

Given the large size of LLM training datasets, ML software frameworks use two common approaches for efficient dataset handling: (1) loading the entire dataset *in-memory* or (2) accessing the dataset outside of memory with *memory mapping*. Although in-memory has an advantage for integrity measurements, frameworks such as Hugging Face adopt and default to using memory-mapped datasets to minimize the memory footprint of large datasets that cannot fit entirely into main memory [32]. Memory mapping also has an advantage over in-memory when running with multiple processes. Since each process can access the same memory-mapped file without duplicating the dataset in memory, the operating system efficiently shares pages among processes. This avoids redundant memory usage and eliminates the need for each worker to load a separate copy of the dataset, which would otherwise increase both memory consumption and startup latency. As a result, memory-mapping provides better scalability and I/O efficiency in multi-process data loading scenarios.

To accurately attest to properties that depend on a dataset, PAL\*M must measure the dataset (or its items) upon use, since  $\mathcal{A}_{\text{Adv}}$  could tamper with data in external storage at any time (recall threat model in Section 3.2). Figure 4 shows how PAL\*M handles this for *in-memory* and *memory-mapped* datasets.

**Case 1: In-memory Dataset.** For integrity measurement,

this is the ideal approach when sufficient TD memory is available. Since the TD memory is protected, data within cannot be tampered. As a result, the dataset can be measured once during loading, as long as it stays in memory for the entire operation. As shown in Figure 4 (left), our framework loads the entire dataset into memory, measures it, and has it available for the program thereafter. Since one hash operation is required, the overhead is minimal (discussed further in Section 6).

**Case 2: Memory-mapped Dataset.** In contrast to the in-memory case, the dataset resides on the disk, and a *memory mapping* data structure resides in memory (see Figure 4: right). As records are sampled from the dataset, the data structure is used to read just the requested data items into memory. Since the dataset stays on disk, it is vulnerable to tampering at run-time, resulting in inconsistencies between what is measured and what is used (i.e., TOCTOU attacks [9]).

To account for this, we measure each record at the time it is sampled, accumulating a measurement of the dataset in use. Since training algorithms often *randomly sample* records, a straightforward approach (e.g., a hash chain over accessed records) would be unsuitable, as different sampling orders would result in different measurements. Based on this insight, we employ an *incremental multiset hash* (MSH) [14].

MSH is a cryptographic primitive that produces a fixed-size hash over an unordered collection. It is suitable for settings in which the order of elements is irrelevant, but integrity and compactness are required. By accumulating an MSH over the sampled records, PAL\*M accurately measures the dataset that is used at run-time, independent of the sampling order. Additionally, this approach has low memory overhead since one multiset hash value is maintained.

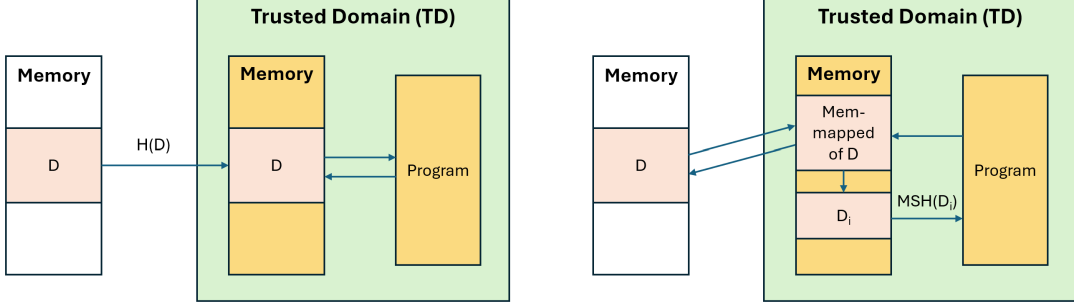


Figure 4: Depiction of PAL\*M’s handling of *in-memory* (left) and *memory-mapped* (right) dataset. In the *in-memory* approach, the entire dataset is loaded and measured once at load time. In the *memory-mapped* approach, individual records are measured when accessed using a multiset hash to ensure consistent measurements regardless of sampling order.

We use the `Mset-Mu-Hash` multiplicative multiset hash construction (from Theorem 2 in [14]) defined below. Let  $B$  denote a set of bit vectors of length  $m$ ,  $M$  a multiset of elements of  $B$ , and  $M_b$  be the number of times  $b \in B$  is in the multiset  $M$ . Let  $h$  be a poly-random function performing  $h : B \rightarrow \mathbb{Z}_n^l$ , given  $n = 2^{\sqrt{m}}$  and  $l = \sqrt{m}$ . The multiplicative multiset hash  $MSH(M)$  is defined as:

$$MSH(M) = \sum_{b \in B} M_b h(b) \mod n$$

Compared to straightforward dataset hashing, this approach incurs additional overhead due to iterative hash and modular operations. However, this overhead is negligible compared to computation-heavy ML tasks (shown in Section 6).

It is possible that expected dataset measurement from  $Tr$  is not  $MSH$ . Consequently, when memory-mapped datasets are in use, PAL\*M must also enable methods for  $Vrf$  to trace back to original dataset measurements.

### 4.3 Property Measurements for Large Generative Models

Recall from Section 3.1 that obtaining property attestation evidence requires (1) obtaining measurements of  $\{op, I, O\}$  and (2) reporting those measurements by producing an authentication token. In this section, we discuss the former.

We categorize properties measured by PAL\*M as one of the following based on  $op$ : dataset property, model property, model interaction property. Based on this, we focus on the following components of property measurement (subset of those from Section 3.1):

- **Input ( $I$ ):** inputs (e.g., datasets, models, queries, or other parameters) used by  $op$ .
- **Output ( $O$ ):** outputs (e.g., prompt response, model, and dataset) produced by  $op$ ;
- **Property:** an expression that describes semantics (either natural language or mathematical expression) of the relationship between  $\{op, I, O\}$ .
- **Attestation Measurement ( $Att$ ):** Measurements that reflects the property under the system and adversary model (from

Table 1: Notation Summary

Symbol	Definition
$I, O, Att$	Set of inputs, outputs, and attestation measurements
$P_{dist}$	Distributional property
$MSH$	Multiset hash function
$h$	Standard cryptographic hash function (e.g., SHA3)
$h_D$	Dataset hash (either $MSH$ or $h$ based on memory management strategy from Sec. 4.2)
$GPU_{att}$	Attestation token from TEE GPU
$\mathcal{D}$	Dataset
$\mathcal{D}_{tr}$	Training dataset
$\mathcal{D}_{pre}$	Preprocessed dataset
$\mathcal{M}_{ar}$	Model architecture
$\mathcal{T}$	Training configuration
$\mathcal{M}_{tr}$	Pretrained model
$\mathcal{M}_{tok}$	Tokenizer
$id_{opt}$	Optimization type
$\mathcal{M}_{adp}$	Adapter model
$\mathcal{D}_{opt}$	Optimization dataset
$[\cdot]^*$	Optional components
$\mathcal{D}_{te}$	Test dataset
$metric$	Evaluation metric
$q_i, r_i$	The $i$ -th inference query and response
$\mathcal{H}$	Session history (i.e., set of all query-response pairs $[(q_0, r_0), \dots, (q_{i-1}, r_{i-1})]$ ) that are used as additional context to produce $q_i$ for $r_i$

Section 3.1 and 3.2).

**Note:** For all operations that require  $GPU$ ,  $Att$  must include  $GPU_{att}$  to reflect the complete environment in which the computations were performed. Therefore,  $GPU_{att}$  is included as an optional input (denoted with  $[\cdot]^*$ ) for all operations described in this section. A summary of frequent notation in this section is in Table 1.

#### 4.3.1 Dataset Properties

We focus on dataset properties based on the following operations: dataset preprocessing, calculation of dataset attribute distribution calculation, and dataset measurement binding.

Dataset preprocessing (from Section 2) may occur prior to training or inference. We define attestation measurement for preprocessing in Definition 1. For preprocessing,  $I$  contains an input dataset ( $\mathcal{D}$ ) and  $O$  contains an output pre-processed

dataset ( $\mathcal{D}_{pre}$ ). A property measurement of preprocessing asserts that  $\mathcal{D}_{pre}$  was the result of computing a preprocessing algorithm (PreProc) on  $\mathcal{D}$ . Finally,  $Att$  contains measurements of  $\mathcal{D}$  and  $\mathcal{D}_{pre}$  using the dataset hash function ( $h_{\mathcal{D}}$ ): either a standard cryptographic hash function ( $h$ ) or a MSH, based on whether  $\mathcal{D}$  and  $\mathcal{D}_{pre}$  are in-memory or memory mapped, respectively.

---

#### Definition 1: Preprocessing

---

**Input (I):**  $\mathcal{D}$

**Output (O):**  $\mathcal{D}_{pre}$

**Property:**  $\mathcal{D}_{pre} = \text{PreProc}(\mathcal{D})$

**Att. Measurement (Att):**  $h_{\mathcal{D}}(\mathcal{D}), h_{\mathcal{D}}(\mathcal{D}_{pre}), [GPU_{att}]^*$

---

Dataset attribute distribution calculations [16] reflect a distribution of an attribute across a dataset (e.g., word lengths, word frequency for LLMs). We define attestation measurement for calculation of attribute distribution in Definition 2. For this operation,  $I$  contains  $\mathcal{D}$ , and  $O$  contains an attribute distribution ( $A_{dist}$ ).  $Att$ , containing  $h(A_{dist})$  and  $h_{\mathcal{D}}(\mathcal{D})$ , asserts the property that  $A_{dist}$  was obtained by an algorithm (Dist) that computes an attribute's distribution on  $\mathcal{D}$ .

---

#### Definition 2: Attribute Distribution

---

**Input (I):**  $\mathcal{D}$

**Output (O):**  $A_{dist}$

**Property:**  $A_{dist} = \text{Dist}(\mathcal{D})$

**Att. Measurement (Att):**  $h(A_{dist}), h_{\mathcal{D}}(\mathcal{D}), [GPU_{att}]^*$

---

It is possible that reference values offered by Tru are produced by  $h$  while an operation requires memory-mapping, resulting in a measurement based on MSH. To account for this scenario, PAL<sup>\*</sup>M supports measurement binding defined in Definition 3.

---

#### Definition 3: Measurement Binding

---

**Input (I):**  $\mathcal{D}$ ,

**Output (O):**  $h(\mathcal{D}), \text{MSH}(\mathcal{D})$

**Property:**  $h(\mathcal{D})$  and  $\text{MSH}(\mathcal{D})$  were produced from  $\mathcal{D}$

**Att. Measurement (Att):**  $h(h(\mathcal{D}) || \text{MSH}(\mathcal{D})), [GPU_{att}]^*$

---

For measurement binding,  $I$  contains  $\mathcal{D}$ , and  $O$  contains the measurements of  $\mathcal{D}$  that should be bound:  $h(\mathcal{D})$  and  $\text{MSH}(\mathcal{D})$ . A property that  $h(\mathcal{D})$  and  $\text{MSH}(\mathcal{D})$  were produced from the same dataset is asserted through  $Att$  containing  $h(h(\mathcal{D}) || \text{MSH}(\mathcal{D}))$ .

### 4.3.2 Model Properties

**Training Properties.** First, we consider training, building on prior work [17]. We define attestation measurements for training in Definition 4. For training,  $I$  includes the specified model architecture ( $\mathcal{M}_{ar}$ ), training dataset ( $\mathcal{D}_{tr}$ ), training configuration ( $\mathcal{T}$ ), which specifies hyperparameters, and a tokenizer ( $\mathcal{M}_{tok}$ ). Then,  $O$  contains the trained model ( $\mathcal{M}_{tr}$ ).  $Att$  contains measurements of ( $\mathcal{T}, \mathcal{M}_{ar}, \mathcal{M}_{tr}$ ) using  $h$  and  $\mathcal{D}$  using

$h_{\mathcal{D}}$ , asserting a property describing that  $\mathcal{M}_{tr}$  was obtained by a training algorithm (Train) taking  $\mathcal{D}_{tr}, \mathcal{T}, \mathcal{M}_{ar}$ .

---

#### Definition 4: Training

---

**Input (I):**  $\mathcal{M}_{ar}, \mathcal{D}_{tr}, \mathcal{T}, \mathcal{M}_{tok}$

**Output (O):**  $\mathcal{M}_{tr}$

**Property:**  $\mathcal{M}_{tr} = \text{Train}(\mathcal{D}_{tr}, \mathcal{T}, \mathcal{M}_{ar})$

**Att. Measurement (Att):**  $h(\mathcal{M}_{tr}), h(\mathcal{M}_{ar}), h_{\mathcal{D}}(\mathcal{D}_{tr}), h(\mathcal{T}), [GPU_{att}]^*$

---

Definition 5 defines attestation measurements for post-training model optimizations (e.g., fine-tuning, quantization, pruning). For model optimization,  $I$  contains the following required inputs:  $\mathcal{M}, \mathcal{T}, \mathcal{M}_{tok}$ , and the optimization type ( $id_{opt}$ ). Optional components of  $I$  include a base adapter layer ( $\mathcal{M}_{adp}$ ) and additional datasets ( $\mathcal{D}_{opt}$ ). For this operation,  $O$  contains the optimized model ( $\mathcal{M}_{opt}$ ).  $Att$  contains all components of  $I$  and  $O$  using  $h$  and  $h_{\mathcal{D}}$ , reflecting its assertion that:

- Opt is selected from a set of known optimization functions ( $\mathcal{F}_{opt}$ ) based on  $id_{opt}$ ;
- $\mathcal{M}_{opt}$  is the result of Opt taking all components of  $I$ .

---

#### Definition 5: Weight Optimizations

---

**Input (I):**  $\mathcal{M}, \mathcal{M}_{tok}, \mathcal{T}, id_{opt}, [\mathcal{M}_{adp}, \mathcal{D}_{opt}]^*$ ,

**Outputs (O):**  $\mathcal{M}_{opt}$

**Property:**  $\text{Opt} = \mathcal{F}_{opt}[id_{opt}]$

$\mathcal{M}_{opt} = \text{Opt}(\mathcal{M}, \mathcal{M}_{tok}, \mathcal{T}, [\mathcal{M}_{adp}, \mathcal{D}_{opt}]^*)$

**Att. Measurement (Att):**  $h(\mathcal{M}), h(\mathcal{M}_{tok}), h(\mathcal{T}), h(id_{opt}), [GPU_{att}, h(\mathcal{M}_{adp}), h_{\mathcal{D}}(\mathcal{D}_{opt})]^*$

---

**Evaluation Properties.** As described in Section 2, generative models have various benchmarks to produce metrics reflecting a model's effectiveness according to a particular criteria. Attestation measurement for model evaluation is defined in Definition 6. For model evaluation,  $I$  includes  $\mathcal{M}, \mathcal{M}_{tok}$ , and a test dataset ( $\mathcal{D}_{te}$ ), while  $O$  contains the evaluation metric. Measurements of  $\mathcal{M}$  and  $\mathcal{M}_{tok}$  using  $h$  and  $\mathcal{D}_{te}$  using  $h_{\mathcal{D}}$  in  $Att$  assert a property about the evaluation: that metric was produced by an evaluation operation (Eval) taking  $\mathcal{M}, \mathcal{M}_{tok}$ , and  $\mathcal{D}_{te}$ .

---

#### Definition 6: Evaluation

---

**Input (I):**  $\mathcal{M}, \mathcal{M}_{tok}, \mathcal{D}_{te}$

**Output (O):** metric

**Att. Measurement (Att):**  $h(\mathcal{M}), h(\mathcal{M}_{tok}), h_{\mathcal{D}}(\mathcal{D}_{te}), [GPU_{att}]^*$

**Property:**  $\text{metric} \leftarrow \text{Eval}(\mathcal{M}, \mathcal{M}_{tok}, \mathcal{D}_{te})$

---

### 4.3.3 Inference-time Properties

We consider two cases of inference-time properties which includes interactions between client and model: one prompt-response inference and a *chat session* of multiple prompt-response inference pairs.

Attestation for a single inference are defined in Definition 7. A inference query ( $q$ ) is one component of  $I$  along with  $\mathcal{M}$

and  $\mathcal{M}_{tok}$ , while the  $O$  contains the inference response ( $r$ ). Measurements of  $q$ ,  $\mathcal{M}$ ,  $\mathcal{M}_{tok}$ , and  $r$  using  $h$  assert the property that  $q$  was obtained by passing  $r$  first through  $\mathcal{M}_{tok}$  and then through  $\mathcal{M}$ .

---

**Definition 7:** Single Inference

---

**Input ( $I$ ):**  $q, \mathcal{M}, \mathcal{M}_{tok}$

**Output ( $O$ ):**  $r$

**Property:**  $q = \mathcal{M}(\mathcal{M}_{tok}(r))$

**Att. Measurement (Att):**  $h(\mathcal{M}), h(I), h(\mathcal{M}_{tok}), h(q), [GPU_{att}]^*$

---

Attestation reflecting the influence of a chat session on an inference query-response (i.e., a *session inference*) are defined in Definition 8. For a session inference operation,  $I$  contains the same data as the single inference operation, while  $O$  contains  $r$  and the chat session history ( $\mathcal{H}$ ): a sequential list of all  $(q_i, r_i)$  pairs of the current chat session, including  $(q, r)$ . Measurements of  $r$ ,  $\mathcal{H}$ ,  $q$ ,  $\mathcal{M}_{tok}$ , and  $\mathcal{M}$  using  $h$  assert the property that  $r$  was obtained from passing  $q$  prepended with  $\mathcal{H}$  without  $(q, r)$  through  $\mathcal{M}_{tok}$ , followed by passing that result through  $\mathcal{M}$ .

---

**Definition 8:** Session Inference

---

**Input ( $I$ ):**  $q, \mathcal{M}_{tok}, \mathcal{M}$

**Output ( $O$ ):**  $r, \mathcal{H}$

**Property:**  $r = \mathcal{M}(\mathcal{M}_{tok}(\mathcal{H} \setminus [q, r] \parallel q))$

**Att. Measurement (Att):**  $h(r), h(\mathcal{H}), h(q), h(\mathcal{M}_{tok}), h(\mathcal{M}), [GPU_{att}]^*$

---

## 4.4 From Measurement to Attestation

For each  $op$ , the corresponding components of  $Att$ , as defined in Section 4.3, are used to construct property attestation evidence. We refer to each property attestation as *proof of  $<op>$* . A table of operations and resulting property attestations is shown in Appendix A. In this section, we describe how PAL\*M interacts with other system components and leverages Intel TDX features to respond to  $Inr$  requests and convert its property measurements into attestation evidence.

Figure 5 shows the property attestation protocol enabled by PAL\*M. Here, we describe the interactions between  $Inr$  and  $Prv$  containing a VMM (including QE), TDX module, and PAL\*M-based TD. We note there are several possible interactions between  $Inr$  and  $Vrf$  (e.g.,  $Inr$  publishes attestations to a *transparency log* [24, 62]). We discuss implications of alternative strategies in Section 8.

In an offline phase,  $Prv$  initializes and measures the PAL\*M TD. In step (1), VMM specifies the TD image that should be used. In step (2), the Intel TDX architecture and TDX module measure the TD image into  $h_{TD}$  and launch it.

After initialization, the online protocol can begin. In step (1),  $Inr$  sends a property attestation request to  $Prv$  containing  $op$ , an attestation challenge ( $Chal$ ), and a set of input assets ( $I$ ). For large input assets (e.g., datasets or models),

$Inr$ 's request may specify repositories from which  $Prv$  should download them. Or,  $Inr$ 's request may specify that  $Prv$  use a dataset/model owned by  $Prv$ . Regardless of these specificities,  $Prv$  saves all data from the request to disk in step (2) upon receipt. In step (3), the PAL\*M TD imports request data and all data required for  $op$  into its memory. Datasets are imported depending on whether  $Prv$  is using a memory-mapped or an in-memory dataset (from Section 4.2).

PAL\*M TD reads  $op$  to execute the corresponding function in step (4). During execution, it obtains a set of input measurements ( $\mathcal{H}_I$ ). After completing the operation, PAL\*M will obtain a set of outputs ( $O$ ) and corresponding measurements ( $\mathcal{H}_O$ ) in step (5).  $\mathcal{H}_I$  and  $\mathcal{H}_O$  correspond to components of  $Att$  for each  $op$  described in Section 4.3.

Next, PAL\*M prepares the request for TDREPORT generation in step (6). To do so, it assigns REPORTDATA input used in TDREPORT generation (recall Section 2.2) as the concatenation of  $\{Chal, \mathcal{H}_I, \mathcal{H}_O\}$ . Upon receiving REPORTDATA, the TDX module will create a TDREPORT in step (7) by invoking the CPU. During this step, the CPU will compute a MAC over  $h_{TD}$ , measurements of the TDX module, and all data extended into REPORTDATA by PAL\*M. In step (8), the MAC-ed TDREPORT is passed to VMM, who passes it to QE in step (9).

Upon receiving the MAC-ed TDREPORT, QE performs the following actions:

- checks that the MAC on the TDREPORT is valid, to ensure VMM did not tamper with the TDREPORT it received from the TDX Module;
- uses TDREPORT to produce the QUOTE containing all measurements from TDREPORT plus a signature ( $sig$ ).

In step (10),  $Prv$  sends QUOTE and optionally  $O$  (if it is not confidential) to  $Inr$ , who sends them to  $Vrf$  in step (11).

Upon receiving QUOTE and (optionally)  $O$  from  $Inr$ ,  $Vrf$  parses the response to perform verification. First, it checks  $sig$  to determine whether the QUOTE came from  $Prv$ . Next, it checks  $Chal$  to determine the freshness of the response. The type of  $Chal$  that is effective depends on the operation. We discuss methodology to select  $Chal$  in Section 8.

Assuming both checks pass,  $Vrf$  continues to inspect the measurements of the TD image, TDX module image, and  $GPU_{att}$  (by obtaining reference values from Intel and NVIDIA). Assuming this passes,  $Vrf$  continues to inspecting  $\mathcal{H}_I$ ,  $\mathcal{H}_O$ , and  $O$ . If  $O$  and was sent to  $Vrf$ , it checks whether  $\mathcal{H}_O$  corresponds to  $O$ . Finally,  $Vrf$  inspects  $\mathcal{H}_I$  and  $\mathcal{H}_O$ , consulting reference values from  $Tru$  as needed, to determine if the desired property related to  $op$  is upheld.

## 5 Experiment Setup

### 5.1 Datasets and Models

We use the following datasets in our experiments:

- **BookCorpus** [74]: a collection of 74 million unpublished novels. We use the full **BookCorpus** dataset for proof of

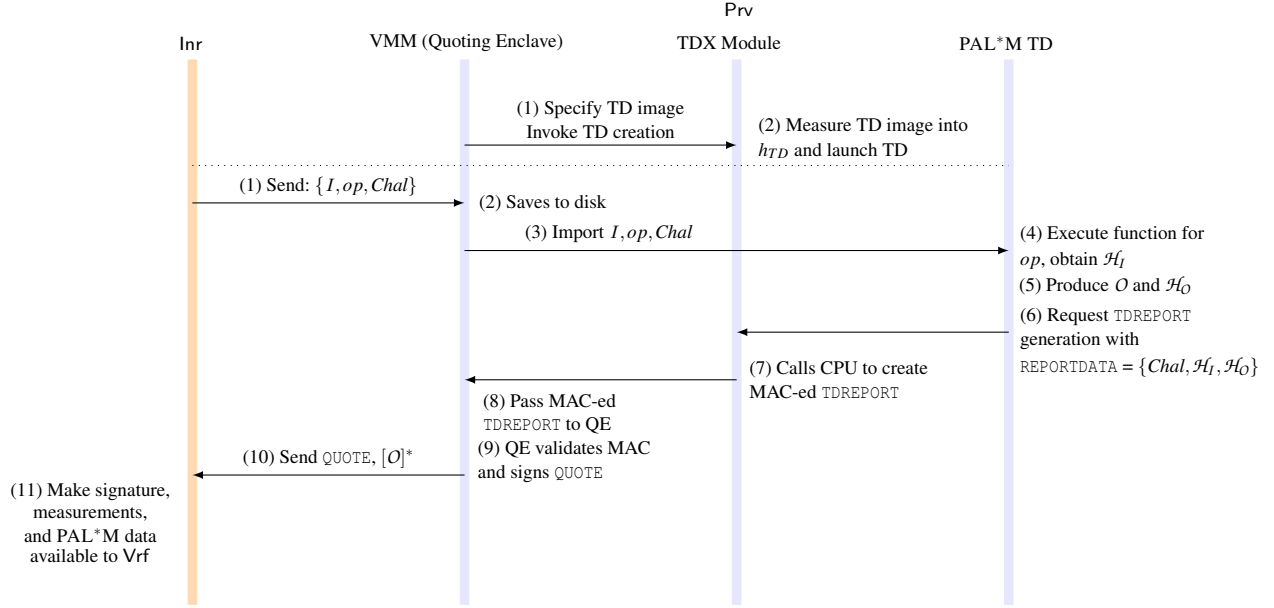


Figure 5: PAL\*M Property Attestation Protocol between **Inr** and **Prv**. Inr sends request to Prv containing untrusted VMM, Quoting Enclave, trusted TDX Module, and attested PAL\*M TD. Prv responds after performing the requested operation, measuring relevant inputs and outputs, and generating both a TDREPORT and QUOTE.

training and attribute distribution, while for proof of pre-processing and proof of binding, we use a 1/100 subset to reduce experiment running time. For training, we pre-process the full **BookCorpus** dataset by tokenizing and concatenating text into sequences of 1024 tokens.

- **yahma/alpaca-cleaned** [65]: a instruction-following dataset containing over 52,000 instruction-response pairs aimed at improving model alignment. We use this dataset for proof of fine-tuning (one type of proof of optimization) to provide a dataset variety other than **BookCorpus**.
- **MMLU** [27]: a multiple-choice question-and-answer (Q&A) dataset used to test a model’s knowledge and reasoning across 57 fields. It is widely used to assess general-purpose intelligence in language models. We use all 57 fields for our proof of evaluation experiments.
- **WMT14 (DE – EN)** [8]: a test set of WMT14 German-English to evaluate LLM translation capability. This dataset is used to calculate the BLEU score for our proof of evaluation experiment.
- **CoQA** [54]: a conversational Q&A dataset containing stories paired with context-dependent questions/answers. For proof of inference, we select the first question from the first ten records. For the proof of session inference, we use all ten records and select the first five questions from each, thus simulating a session with 50 prompts.

For models, we use **GPT-2** [52] for proof of training. For fine-tuning, inference, and evaluation, we use three popular instruction-tuned LLMs: **Llama-3.1-8B** [67], **Gemma-3-4B** [66], and **Phi-4-Mini** [2]. We choose

**Llama-3.1-8B** for its 8 billion parameters, while both **Gemma-3-4B** and **Phi-4-Mini** have 4 billion parameters, allowing us to show how the overhead of PAL\*M varies across different model sizes and architectures. To demonstrate a realistic fine-tuning workflow, we fine-tune all three models with LoRA. For quantization, we focus on **Llama-3.1-8B**.

## 5.2 Metrics

We use the following metrics to capture both the overall overhead from PAL\*M and the main sources of overhead:

- **Total Time:** The total execution time spent on the task.
- **Baseline:** The baseline represents running the task on a TDX-enabled machine without any measurement or attestation from PAL\*M. We omit the baseline for running our framework on non-TDX machines because the overhead of TDX compared to non-TDX systems has already been studied [13]. Our focus is solely on the overhead introduced by our framework in the environment where it is intended to be used.
- **Memory Usage (GB):** The memory usage of the system during the operation.
- **Input Measurement Time:** The time spent hashing the inputs. For memory-mapped datasets, this is the time spent performing MSH when records are accessed.
- **Output Measurement Time:** The time spent hashing the outputs (e.g., model, dataset, or result from the task).
- **Attestation:** The time spent by Intel TDX and NVIDIA H100 to produce QUOTE and  $GPU_{att}$ , respectively.

Table 2: Performance for proofs of dataset attribute distribution, preprocessing, and binding using **BookCorpus** (Full) and **BookCorups** (1/100).

Proof of	Attribute Distribution		Preprocessing		Binding
Dataset Memory Variant	BookCorpus (Full)		BookCorpus (1/100)		N/A
	In-memory	Memory-mapped	In-memory	Memory-mapped	
<b>Total Time</b>	339.16 min	577.45 min	237.70 s	380.16 s	339.62 s
<b>Baseline</b>	339.09 min	185.06 min	236.66 s	141.51 s	102.41 s
<b>Mem Usage (GB)</b>	5.47	3.96	0.12	0.04	0.14
<b>Input Meas.</b>	3.06 s	392.37 min	0.04 s	237.70 s	236.22 s
<b>Output Meas.</b>	0.53 ms	0.52 ms	0.10 s	0.10 s	0.04 ms
<b>Attestation</b>	1.06 s	1.02 s	0.90 s	0.85 s	0.99 s
<b>Meas. Overhead (%)</b>	0.015	67.95	0.06	62.55	69.55
<b>Att. Overhead (%)</b>	0.0029	0.0052	0.38	0.22	0.29

- **Measurement Overhead (%)**: The total measurement overhead from  $\text{PAL}^*M$  as a percentage of the total time.
- **Attestation Overhead (%)**: The total attestation overhead from  $\text{PAL}^*M$  as a percentage of the total time.

### 5.3 Prototype Configuration

All experiments were conducted on a TD configured with 32 vCPUs and 128 GB of memory, running Ubuntu 24.04.1 LTS with kernel version 6.8.0-86-generic [12]. The host machine is equipped with an Intel Xeon Silver 4514Y processor, 512 GB of RAM, and an NVIDIA H100 NVL 94 GB GPU with confidential compute mode enabled [48]. We assign the GPU directly to the TD using Direct Device Assignment (DDA) to give the TD full access to the GPU. We run each experiment five times and report the average. Standard deviation was negligible in all cases, thus we exclude from the tables.

$\text{PAL}^*M$  is implemented in Python and provides two primary functionalities: (1) input/output measurement, and (2) attestation using Intel Data Center Attestation Primitives (DCAP) [58] and NVIDIA Remote Attestation Service (NRAS) [49].  $\text{PAL}^*M$  is built on PyTorch and the Hugging Face Datasets framework, allowing access to both dataset and model internals for measurement. For attestation, we use Intel DCAP to generate QUOTE and NRAS to verify  $GPU_{att}$ .

We also use the following operation-specific frameworks for the experiments:

- **Unsloth** [15]: an open-source framework that provides optimized, memory-efficient fine-tuning for large language models. We use it for proof of fine-tuning experiment.
- **AutoAWQ framework** [26]: implements the Activation-aware Weight Quantization (AWQ) algorithm for quantizing LLMs. We use it for proof of quantization experiment.
- **Im-evaluation-harness framework** [22]: standardized toolkit that runs language models on multiple benchmark tasks through a unified API to produce comparable scores. We use it for proof of evaluation, specifically evaluating the model with **MMLU**.

Table 3: Performance for proof of training with **GPT-2** on tokenized and preprocessed **BookCorpus**.

Dataset Memory Variant	BookCorpus (Full)	
	In-memory	Memory-mapped
<b>Total Time</b>	387.86 min	410.85 min
<b>Baseline</b>	387.79 min	387.58 min
<b>Mem Usage (GB)</b>	2.74	0.04
<b>Input Meas.</b>	1.88 s	23.24 min
<b>Output Meas.</b>	1.14 s	1.14 s
<b>Attestation</b>	1.00 s	0.96 s
<b>Meas. Overhead (%)</b>	0.01	5.66
<b>Att. Overhead (%)</b>	0.004	0.004

## 6 Evaluation

### 6.1 R1: Efficient

Tables 2-6 show the timing results for the performance evaluations. The cells in gray represent the baseline,  $\text{PAL}^*M$ 's overhead is highlighted in blue, and the total times are in orange. We also parallelize the dataset lookup iterations across 8 cores for all experiments that require manual dataset iteration for dataset-related attestations.

**Dataset Attestations.** Table 2 presents the results for all dataset attestations. While the measurement overhead of the memory-mapped approach from our framework appears large relative to the total compute time, dataset attestations correspond to operations that will likely occur once:

- proof of attribute distribution and preprocessing are relevant for any future use of a particular dataset;
- proof of binding is relevant for any MSH produced in the future.

The actual computation for these dataset-related tasks is not expensive compared to training and evaluation tasks. Thus, the observed 62% to 70% reflects the raw overhead from hashing, since the baseline workloads are minimal for calculating an attribute distribution and preprocessing. As for binding, the main overhead comes from iterating through the dataset to compute the MSH for all records. The input measurement time for iterating through the dataset is similar to the proof of preprocessing experiment, demonstrating consistent measurement time when the dataset remains the same.

Since the dataset is processed in parallel, the baseline time for the memory-mapped approach is much lower than that of the in-memory approach. Due to the nature of memory mapping, parallel I/O scales better since all processes can directly access the same underlying memory pages without duplication. In contrast, the in-memory approach requires each process to load or copy portions of the dataset into its own address space, which introduces additional memory copying and increases overhead.

**Model Attestations.** In contrast to dataset attestations, the

Table 4: Performance for proof of model optimization (fine-tuning and quantization).

Proof of	Fine-tuning								Quantization
Model	Llama-3.1-8B				Gemma-3-4B				Phi-4-Mini
Memory Variant	In-memory	Memory-mapped	In-memory	Memory-mapped	In-memory	Memory-mapped	In-memory	Memory-mapped	N/A
<b>Total Time</b>	268.81 min		269.15 min		325.61 min		325.31 min		169.93 min
<b>Baseline</b>	268.30 min		266.62 min		325.29 min		322.94 min		169.65 min
<b>Mem Usage (GB)</b>	0.085		0.004		0.087		0.004		0.088
<b>Input Meas.</b>	28.76 s		151.01 s		17.93 s		140.90 s		15.83 s
<b>Output Meas.</b>	0.30 s		0.30 s		0.23 s		0.23 s		0.06 s
<b>Attestation</b>	1.11 s		1.01 s		1.00 s		1.27 s		1.00 s
<b>Meas. Overhead (%)</b>	0.18		0.94		0.09		0.72		1.35
<b>Att. Overhead (%)</b>	0.007		0.006		0.005		0.006		0.011
									4.70
									0.117

Table 5: Performance for proof of evaluation based on **MMLU** and BLEU score with **WMT14 (DE-EN)** dataset.

Model	Llama-3.1-8B				Gemma-3-4B				Phi-4-Mini			
	In-memory		Memory-mapped		In-memory		Memory-mapped		In-memory		Memory-mapped	
Metric	MMLU	BLEU	MMLU	BLEU	MMLU	BLEU	MMLU	BLEU	MMLU	BLEU	MMLU	BLEU
<b>Total Time</b>	18.50 min	121.71 min	19.59 min	121.55 min	15.10 min	242.23 min	16.21 min	241.53 min	12.11 min	119.03 min	13.21 min	118.65 min
<b>Baseline</b>	18 min	121.23 min	18.03 min	120.94 min	14.79 min	241.92 min	14.83 min	241.10 min	11.83 min	118.75 min	11.86 min	118.26 min
<b>Mem Usage (GB)</b>	0.028	0.001	0.013	0.001	0.022	0.001	0.008	0.001	0.025	0.001	0.009	0.001
<b>Input Meas.</b>	28.76 s	28.16 s	92.99 s	35.57 s	17.53 s	17.32 s	81.82 s	24.55 s	15.65 s	15.65 s	79.96 s	22.50 s
<b>Output Meas.</b>	0.11 s	0.038 ms	0.11 s	0.035 ms	0.11 s	0.033 ms	0.11 s	0.035 ms	0.11 s	0.036 ms	0.11 s	0.035 ms
<b>Attestation</b>	0.85 s	1.10 s	0.97 s	1.07 s	0.84 s	1.12 s	0.83 s	1.23 s	0.79 s	1.08 s	0.87 s	1.13 s
<b>Meas. Overhead (%)</b>	2.60	0.39	7.92	0.49	1.95	0.12	8.42	0.17	2.17	0.22	10.11	0.31
<b>Att. Overhead (%)</b>	0.08	0.015	0.08	0.015	0.09	0.008	0.09	0.009	0.11	0.015	0.11	0.016

measurement overhead of our PAL<sup>\*M</sup> for proof of training in the memory-mapped case is only 5.66% of the total time (Table 3). LLM training is computationally expensive; hence, the measurement time results in a smaller overhead compared to the total computation.

As for model optimization, similar to training, proof of fine-tuning (Table 4) also shows minimal overhead of  $\leq 1.35\%$  across all models, plus a substantial reduction in memory usage from 85-87 MB to only 4 MB. For proof of quantization, since no dataset is involved, the 4.7% overhead comes from measuring models.

As shown in Table 5, overheads for proof of evaluation with the MMLU benchmark are 3.81-5.06% for the in-memory case and 10.03-11.84% for the memory-mapped case (Table 5). For BLEU score, since dataset access is limited (since the **WMT14 (DE-EN)** contains only 3003 records), the overhead of performing MSH in the memory-mapped case is comparable to hashing the dataset in the in-memory case, with the total overhead remaining  $\leq 1.0\%$  across all models.

**Inference Attestations.** Table 6 presents the results for both proof of inference and proof of session inference. For proof of inference, measurement overhead is large due to time required to measure the model, while the attestation overhead remains similar to previous cases. This follows the same pattern observed in dataset-related attestations where the over-

head appears large (64.34% for **Llama-3.1-8B**, around 43.28% for **Gemma-3-4B**, and 52.16% for **Phi-4-Mini**) because the underlying computation is relatively small. This represents an extreme case in which both measurement and attestation are performed for only one prompt.

On the other hand, for proof of session inference, we perform attestation only once after all interactions with the model have completed. This simulates a more realistic user-model interaction, with previous prompts and responses forming the context with a single attestation for the entire session. In this setting, the measurement overhead is significantly smaller, 11.03% for **Llama-3.1-8B**, 3.57% for **Gemma-3-4B**, and 6.28% for **Phi-4-Mini**.

## 6.2 R2-3: Scalable & Versatile

**Scalability.** Attestations can be generated by Prv running on any hardware that supports and is configured for confidential computing. PAL<sup>\*M</sup> can apply to any CVM-GPU configuration given both have TEEs. While widespread use of Intel TDX and NVIDIA confidential computing remains limited at the time of writing, more cloud service providers, such as Microsoft Azure, have begun supporting confidential VMs with NVIDIA H100 GPUs [25]. Although GPU-based confidential computing is currently available only on NVIDIA Hopper and

Table 6: Performance of proof of inference for one query-response and proof of session inference for 50 query-responses.

Model Proof of Inference Type	Llama-3.1-8B		Gemma-3-4B		Phi-4-Mini	
	Single	Session	Single	Session	Single	Session
<b>Total Time</b>	43.31 s	256.19 s	40.55 s	489.69 s	29.94 s	249.37 s
<b>Baseline</b>	14.54 s	227.02 s	22.09 s	471.22 s	13.40 s	232.70 s
<b>Mem Usage (GB)</b>	0.001	0.001	0.001	0.001	0.001	0.001
<b>Input Meas.</b>	27.17 s	28.25 s	16.27 s	17.47 s	14.59 s	15.66 s
<b>Output Meas.</b>	0.042 ms	0.092 ms	0.038 ms	0.103 ms	0.040 ms	0.117 ms
<b>Attestation</b>	0.75 s	0.92 s	0.79 s	0.99 s	0.71 s	1.01 s
<b>Meas. Overhead (%)</b>	64.34	11.03	43.28	3.57	52.16	6.28
<b>Att. Overhead (%)</b>	2.09	0.36	2.24	0.20	3.10	0.41

Blackwell GPUs [47], which are high-end devices, we expect this technology to be adopted more broadly in future GPU generations. Verification of PAL<sup>\*</sup>M attestation evidence can be performed by any Vrf that knows corresponding public keys for Prv’s attesting devices. Thus, PAL<sup>\*</sup>M satisfies **R2**.

**Versatility.** PAL<sup>\*</sup>M satisfies **R3** as PAL<sup>\*</sup>M’s measurement is a software-based approach that relies only on Intel TDX and the NVIDIA H100 for isolation. Therefore, PAL<sup>\*</sup>M can be adapted to any type models or dataset, beyond those used in our experiments. Additionally, property attestations can also be easily added by extending PAL<sup>\*</sup>M with additional measurer scripts corresponding to the new property, with no changes required by Inr or Vrf.

### 6.3 R4: Secure

Based on the threat model outlined in Section 3,  $\mathcal{A}dv$  has control over the host machine and VMM. As a result,  $\mathcal{A}dv$  can attempt to (1) tamper with any operation inputs; (2) tamper, discard, or replay TDREPORT or QUOTE at any stage of their construction or transmission; or (3) tamper with the configuration of PAL<sup>\*</sup>M TD.

$\mathcal{A}dv$  may manipulate  $op$  to change the requested function or misconfigure assets in  $I$  used for the requested function. Both cases are detectable by Vrf, since PAL<sup>\*</sup>M does not measure either until they are loaded into TD-protected memory. Therefore, Vrf is ensured that the inputs reflected in the QUOTE were used in the process. In the case of a memory-mapped data structure,  $\mathcal{A}dv$  may manipulate data before it is read into the TD memory. For example, they may aim to repeat or replace data records during fine-tuning to make the resulting model unfair/biased. However, these attempts can be detected by Vrf, since PAL<sup>\*</sup>M in this case measures records as they are sampled. Even in the case of random sampling, use of MSH ensures Vrf can always determine when the entire dataset was used without replacing or repeating records.

$\mathcal{A}dv$  may attempt to generate false outputs and corresponding measurements in an attempt to create a faulty TDREPORT before it is passed to the QE. However, this is infeasible be-

cause a MAC is computed on the TDREPORT with a key that is inaccessible to software [4], and QE verifies this MAC before generating a QUOTE. Therefore, it is computationally infeasible for  $\mathcal{A}dv$  to forge the MAC-ed TDREPORT. Similarly,  $\mathcal{A}dv$  may attempt to forge the QUOTE, but this is also infeasible since QUOTE is signed using a provisioned key whose private key material never leaves QE. Finally,  $\mathcal{A}dv$  may attempt to replay responses from the same  $op$  to Vrf, but this is detectable by Vrf due to the inclusion of *Chal* in the construction QUOTE.

Finally, since  $\mathcal{A}dv$  has control over VMM, they can assign which image is used for loading. Therefore, they could load an image containing a backdoor to assist with lying about datasets/models that are used for a particular operation. However, the TD image is measured by the TDX module before TD creation, and included in the QUOTE obtained by Vrf. Therefore, these attempts are detectable by Vrf. Furthermore,  $\mathcal{A}dv$  may attempt to assign a GPU without a TEE to the TD. In this case, Vrf detects it due to PAL<sup>\*</sup>M including GPU attestation evidence when the GPU is used in obtaining outputs. In this case, Vrf would observe  $GPU_{att}$ ’s absence from the response.

Under the assumed threat model,  $\mathcal{A}dv$  cannot evade or generate false outputs with corresponding measurements without detection. Therefore, PAL<sup>\*</sup>M satisfies **R4**.

## 7 Related Work

**Cryptographic Attestations.** Secure multi-party computation (SMPC) and zero-knowledge proofs (ZKPs) have been used to verify ML operations. SMPC has been explored for distributional property attestation but requires per-attestation interaction with a verifier, which is not scalable [16]. Arc uses SMPC with publicly verifiable commitments to bind training and inference for auditing [43]. ZKPs can provide verifiability for training simple ML models (e.g., logistic regression) [23] and neural networks [1], and LLM fine-tuning [56]. ZKPs have also been used for proof of inference across different types of ML models (including LLMs) [31, 41, 63]. Furthermore, ZKPs can help verify security properties of ML models such as differential privacy [20, 61], and fairness [19, 60].

However, these cryptographic primitives have a high computation cost. For instance, it takes around 15 minutes to verify one iteration of VGG11 training [1], making it challenging for practical deployment for applications.

**TEE-based attestations.** Prior works have extensively used TEEs for the confidentiality of data and models [42, 45, 64, 73]. Unlike these approaches, we focus on integrity, leveraging TEEs to attest properties of large generative model operations executed within them. Laminator [17] is the closest related work, using TEEs to attest properties of CPU-only classifier model operations. Schnabl et al. [59] use TEEs to attest the execution of the code, ML model for various inferences, and its outputs. *Atlas* uses TEEs to verify the ML lifecycle by having TEE-equipped contributors attest to the inputs and outputs of artifact creation or transformation and publish these attestations to a transparency log [62]. *VerifiableFL* proposes an integrity-only enclave (called *exclave*), which generates authenticated evidence of input and output data for federated learning [24]. Similar to our approach, it uses CVM technologies (e.g., AMD SEV-SNP), but focuses on federated learning rather than generative models, and it does not focus on addressing the challenges due large datasets outside CVM memory. Rattanavipan and Nunes [53] focus on federated learning by providing stateful proofs of execution that let an external Vrf confirm correct data use, model updates, and local differential privacy on TrustZone-enabled ARM Cortex-M devices. None of these works focus on attesting properties of generative models while accounting for challenges of their computing environments (see Section 3).

## 8 Discussions

**Other Generative Models.** Since PAL\*M is built on PyTorch and Hugging Face, it will work for any model hosted on Hugging Face, including LLMs not used in our experiments and other state-of-the-art generative models, such as diffusion models [28]. As long as the model weights are accessible for measurement, PAL\*M applies. For image generation diffusion models, the attested properties may differ from those of LLMs; for example, the output (and the input, in the case of image-to-image models) is an image during inference. Thus, the required changes are only to the types of inputs and outputs being measured.

**Alternative Designs.** We implemented PAL\*M using Intel TDX in order to take advantage of the confidential computing support of the NVIDIA H100 GPU, which requires the use of a CVM. Another CVM, such as AMD’s SEV-SNP, can be used instead with appropriate driver support, but other TEEs, such as Intel’s SGX, generally lack this support and therefore will not achieve the full performance of PAL\*M. Nevertheless, they can be used for models that have reasonable performance with CPU-only computation, such as in previous work [17].

**Other Data Integrity Techniques.** PAL\*M uses MSH to reduce datasets to a single value that can be computed incre-

mentally as each item is read from storage, yielding the same result irrespective of the order in which the records are used. Nevertheless, the MSH is not without limitations. While the ordering of accesses does not impact the final hash, it is necessary to access each item *exactly once*, leading to unnecessary data accesses whenever a metric does not access the entire dataset. An alternative approach is to use a Merkle tree that allows arbitrary random access within a dataset, at the cost of  $O(\log n)$  additional reads and hash evaluations per lookup. An implementation might use a *proof of binding* to bind a dataset hash to both an MSH and a Merkle tree root hash, allowing it to select a hash type according to the access patterns of the metric being computed.

**Selecting *Chal* in Property Attestation.** Section 4.4 outlines a property attestation protocol enabled by PAL\*M initiated by request from *Inr* containing *Chal*. In conventional RA settings, *Chal* is a nonce or counter used to prevent replay attacks and ensure response freshness. Given ML property attestation in this work is non-interactive with Vrf, selection of *Chal* should be derived from a timestamp rather than a traditional cryptographic nonce or counter.

However, for proof of inference, including a nonce remains valuable to prevent *Prv* from cherry-picking favorable executions. In this setting, Vrf could publish nonce values with associated expiration times for use as PAL\*M attestation challenges. To further mitigate cherry-picking, Vrf may request only proof of session inference, allowing observability of response history (or lack thereof).

## 9 Summary

This work advances ML property attestations by introducing PAL\*M: a practical and comprehensive framework capable of spanning diverse hardware environments (e.g., CPU-GPU), large-scale data, and emerging generative models. We define how to measure properties of generative models and use *incremental multiset hash* functions to capture properties across dataset operations and training. As a result, PAL\*M supports deployable accountability for modern AI systems, laying the groundwork for regulators, developers, and verifiers to reason more concretely about the trustworthiness of ML systems.

**Acknowledgements.** This work is supported in part by the Government of Ontario, the Natural Sciences and Engineering Research Council of Canada (grant number RGPIN-2020-04744), and the Wallenberg Guest Professor Program. The views expressed in the paper are those of the authors and do not reflect the position of the funding agencies.

## References

- [1] Kasra Abbaszadeh et al. Zero-knowledge proofs of training for deep neural networks. In *ACM SIGSAC*

*Conference on Computer and Communications Security*, CCS '24, page 4316–4330, New York, NY, USA, 2024. Association for Computing Machinery.

- [2] Abdelrahman Abouelenin et al. Phi-4-Mini Technical Report: Compact yet Powerful Multimodal Language Models via Mixture-of-LoRAs. *CoRR*, abs/2503.01743, 2025.
- [3] EU Artificial Intelligence Act. The EU Artificial Intelligence Act. *European Union*, 2024.
- [4] Erdem Aktas et al. Intel Trust Domain Extensions (TDX) security review. *Google security review*, 2023.
- [5] AMD. AMD secure encrypted virtualization (sev). <https://www.amd.com/en/developer/sev.html>, 2020.
- [6] Anthropic and Pattern Labs. Confidential inference via trusted virtual machines. <https://www.anthropic.com/research/confidential-inference-trusted-vms>, June 2025. Research report on confidential inference systems using trusted virtual machines.
- [7] ARM. ARM TrustZone for Cortex-A. <https://www.arm.com/technologies/trustzone-for-cortex-a>, 2004.
- [8] Ondrej Bojar et al. Findings of the 2014 Workshop on Statistical Machine Translation. In *Proceedings of the Ninth Workshop on Statistical Machine Translation*, pages 12–58, Baltimore, Maryland, USA, June 2014. Association for Computational Linguistics.
- [9] Sergey Bratus et al. TOCTOU, traps, and trusted computing. In *International Conference on Trusted Computing*, pages 14–32. Springer, 2008.
- [10] Brave Software. Verifiable privacy and transparency: A new frontier for brave ai privacy. <https://brave.com/blog/browser-ai-tee/>, 11 2025. Accessed: 2025-11-26.
- [11] Tom Brown et al. Language Models are Few-Shot Learners. In *Advances in Neural Information Processing Systems*, volume 33, pages 1877–1901. Curran Associates, Inc., 2020.
- [12] Canonical. Canonical TDX Github Repository. <https://github.com/canonical/tdx>, September 2025.
- [13] Marcin Chrąpek et al. Confidential LLM inference: Performance and cost across CPU and GPU TEEs. *arXiv preprint arXiv:2509.18886*, 2025.
- [14] Dwaine Clarke et al. Incremental multiset hash functions and their application to memory integrity checking. In *International conference on the theory and application of cryptology and information security*, pages 188–207. Springer, 2003.
- [15] Michael Han Daniel Han and Unsloth team. Unsloth. <https://github.com/unslothai/unsloth>, 2023.
- [16] Vasisht Duddu et al. Attesting distributional properties of training data for machine learning. In *European Symposium on Research in Computer Security*, pages 3–23. Springer, 2024.
- [17] Vasisht Duddu, Lachlan J Gunn, and N Asokan. Laminator: Verifiable ml property cards using hardware-assisted attestations. In *Proceedings of the Fifteenth ACM Conference on Data and Application Security and Privacy*, pages 317–328, 2024.
- [18] Congyu Fang et al. Proof-of-learning is currently more broken than you think. In *2023 IEEE 8th European Symposium on Security and Privacy (EuroS&P)*, pages 797–816. IEEE, 2023.
- [19] Olive Franzese et al. Secure and confidential certificates of online fairness. In *The Thirty-ninth Annual Conference on Neural Information Processing Systems*, 2025.
- [20] Olive Franzese et al. Secure noise sampling for differentially private collaborative learning. In *Proceedings of the 2025 ACM SIGSAC Conference on Computer and Communications Security*, pages 4649–4663, 2025.
- [21] Leo Gao et al. The Pile: An 800GB Dataset of Diverse Text for Language Modeling. *arXiv preprint arXiv:2101.00027*, 2020.
- [22] Leo Gao et al. The Language Model Evaluation Harness. <https://zenodo.org/records/12608602>, July 2024.
- [23] Sanjam Garg et al. Experimenting with zero-knowledge proofs of training. In *Proceedings of the 2023 ACM SIGSAC Conference on Computer and Communications Security*, CCS '23, page 1880–1894, New York, NY, USA, 2023. Association for Computing Machinery.
- [24] Jinnan Guo et al. ExclaveFL: Providing transparency to federated learning using exacles. *arXiv preprint arXiv:2412.10537*, 2024.
- [25] Krishnaprasad Hande and Microsoft team. General availability: Azure confidential VMs with NVIDIA H100 tensor core GPUs, 2024.
- [26] Casper Hansen. AutoAWQ. <https://github.com/casper-hansen/AutoAWQ>, 2023.
- [27] Dan Hendrycks et al. Measuring Massive Multitask Language Understanding. In *ICLR*. OpenReview.net, 2021.

[28] Jonathan Ho, Ajay Jain, and Pieter Abbeel. Denoising Diffusion Probabilistic Models. In *NeurIPS*, 2020.

[29] Edward J. Hu et al. LoRA: Low-Rank Adaptation of Large Language Models. In *ICLR*. OpenReview.net, 2022.

[30] Yaqi Hu et al. LLM-based misbehavior detection architecture for enhanced traffic safety in connected autonomous vehicles. *IEEE Transactions on Vehicular Technology*, 2025.

[31] Chenyu Huang et al. zkMLaaS: a verifiable scheme for machine learning as a service. In *GLOBECOM 2022-2022 IEEE Global Communications Conference*, pages 5475–5480. IEEE, 2022.

[32] Hugging Face. Datasets Arrow. [https://huggingface.co/docs/datasets/v4.1.1/about\\_arrow](https://huggingface.co/docs/datasets/v4.1.1/about_arrow), 2025. Accessed: 2025-10-01.

[33] Hugging Face. Preprocess. [https://huggingface.co/docs/datasets/en/use\\_dataset](https://huggingface.co/docs/datasets/en/use_dataset), 2025. Accessed: 2025-01-19.

[34] Hugging Face. Trainer. [https://huggingface.co/docs/transformers/main\\_classes/trainer#transformers.Trainer.get\\_train\\_dataloader](https://huggingface.co/docs/transformers/main_classes/trainer#transformers.Trainer.get_train_dataloader), 2025. Accessed: 2025-01-15.

[35] Intel. Intel Provisining Certification Service for ECDSA Attestation. <https://api.portal.trustedservices.intel.com/provisioning-certification>.

[36] Intel. Intel Software Guard Extensions (Intel SGX). <https://www.intel.com/content/www/us/en/developer/tools/software-guard-extensions/overview.html>, 2015.

[37] Intel. Intel Trust Domain Extensions (Intel TDX). <https://www.intel.com/content/www/us/en/developer/tools/trust-domain-extensions/overview.html>, 2023.

[38] Intel. Intel Trust Domain Extensions (Intel TDX) module base architecture specification. <https://cdrrdv2-public.intel.com/853286/intel-tdx-module-base-spec-348549006.pdf>, Apr 2025.

[39] Insu Jang et al. Heterogeneous isolated execution for commodity GPUs. In *Proceedings of the Twenty-Fourth International Conference on Architectural Support for Programming Languages and Operating Systems*, pages 455–468, 2019.

[40] ARM Limited. Overview: Realms. <https://learn.arm.com/learning-paths/servers-and-cloud-computing/cca-container/overview/>.

[41] Tianyi Liu, Xiang Xie, and Yupeng Zhang. zkCNN: Zero knowledge proofs for convolutional neural network predictions and accuracy. In *Proceedings of the 2021 ACM SIGSAC Conference on Computer and Communications Security*, pages 2968–2985, 2021.

[42] Ziyu Liu et al. MirrorNet: A TEE-friendly framework for secure on-device DNN inference. In *2023 IEEE/ACM International Conference on Computer Aided Design (ICCAD)*, pages 1–9. IEEE, 2023.

[43] Hidde Lycklama et al. Holding secrets accountable: Auditing privacy-preserving machine learning. In *USENIX Security Symposium*, 2024.

[44] Sourab Mangrulkar et al. PEFT: State-of-the-art Parameter-Efficient Fine-Tuning methods. <https://github.com/huggingface/peft>, 2022.

[45] Fan Mo et al. DarkneTZ: towards model privacy at the edge using trusted execution environments. In *International Conference on Mobile Systems, Applications, and Services*, MobiSys '20, page 161–174, New York, NY, USA, 2020. Association for Computing Machinery.

[46] Ivan De Oliveira Nunes et al. Toward remotely verifiable software integrity in resource-constrained iot devices. *IEEE Communications Magazine*, 62(7):58–64, 2024.

[47] NVIDIA. AI Security With Confidential Computing. <https://www.nvidia.com/en-us/data-center/solutions/confidential-computing/>.

[48] NVIDIA. NVIDIA Deployment Guide for SecureAI. <https://docs.nvidia.com/cc-deployment-guide-tdx.pdf>, February 2025.

[49] NVIDIA. NVIDIA attestation. <https://docs.nvidia.com/attestation/index.html>, [Accessed] 2025.

[50] OpenAI. Reimagining secure infrastructure for advanced ai. <https://openai.com/index/reimagining-secure-infrastructure-for-advanced-ai/>, 5 2024. Accessed: 2025-11-26.

[51] PyTorch. torch.utils.data — PyTorch 2.9 documentation. <https://docs.pytorch.org/docs/stable/data.html>, 2025. Accessed: 2026-01-15.

[52] Alec Radford et al. Language models are unsupervised multitask learners. *OpenAI blog*, 1(8):9, 2019.

[53] Norrathep Rattanavipanon and Ivan De Oliveira Nunes Nunes. SLAPP: Poisoning prevention in federated learning and DP via stateful proofs of execution. *IEEE Transactions on Information Forensics and Security (TIFS)*, 2025.

[54] Siva Reddy, Danqi Chen, and Christopher D. Manning. CoQA: A conversational question answering challenge. *Transactions of the Association for Computational Linguistics*, 7:249–266, 2019.

[55] Herbert Robbins and Sutton Monro. A stochastic approximation method. *The annals of mathematical statistics*, pages 400–407, 1951.

[56] Bidhan Roy, Peter Potash, and Marcos Villagra. ZK-LoRA: Efficient zero-knowledge proofs for LoRA verification. In *Championing Open-source DEvelopment in ML Workshop @ ICML25*, 2025.

[57] Ahmad-Reza Sadeghi and Christian Stüble. Property-based attestation for computing platforms: caring about properties, not mechanisms. In *Proceedings of the 2004 workshop on New security paradigms*, pages 67–77, 2004.

[58] Vinnie Scarlata et al. Supporting third party attestation for Intel SGX with Intel data center attestation primitives. *White paper*, 12, 2018.

[59] Christoph Schnabl et al. Attestable audits: Verifiable AI safety benchmarks using trusted execution environments. In *ICML Workshop on Technical AI Governance (TAIG)*, 2025.

[60] Ali Shahin Shamsabadi et al. Confidential-PROFIT: Confidential PROof of fair training of trees. In *The Eleventh International Conference on Learning Representations*, 2023.

[61] Ali Shahin Shamsabadi et al. Confidential-DPproof: Confidential proof of differentially private training. In *The Twelfth International Conference on Learning Representations*, 2024.

[62] Marcin Spoczynski, Marcela S. Melara, and Sebastian Szyller. Atlas: A framework for ML lifecycle provenance & transparency. In *2025 IEEE European Symposium on Security and Privacy Workshops (EuroS&PW)*, pages 448–461. IEEE, 2025.

[63] Haochen Sun, Jason Li, and Hongyang Zhang. zkLLM: Zero knowledge proofs for large language models. In *Proceedings of the 2024 on ACM SIGSAC Conference on Computer and Communications Security*, pages 4405–4419, 2024.

[64] Tong Sun et al. TensorShield: Safeguarding on-device inference by shielding critical DNN tensors with TEE. In *ACM SIGSAC Conference on Computer and Communications Security (CCS)*, 2025.

[65] Rohan Taori et al. Stanford Alpaca: An instruction-following llama model. [https://github.com/tatsu-lab/stanford\\_alpaca](https://github.com/tatsu-lab/stanford_alpaca), 2023.

[66] Gemma Team. Gemma 3 Technical Report. *CoRR*, abs/2503.19786, 2025.

[67] Llama Team. The Llama 3 Herd of Models. *CoRR*, abs/2407.21783, 2024.

[68] Florian Tramer and Dan Boneh. Slalom: Fast, verifiable and private execution of neural networks in trusted hardware. In *International Conference on Learning Representations*, 2019.

[69] Ehsan Ullah et al. Challenges and barriers of using large language models (LLM) such as ChatGPT for diagnostic medicine with a focus on digital pathology—a recent scoping review. *Diagnostic pathology*, 19(1):43, 2024.

[70] Ashish Vaswani et al. Attention is all you need. *Advances in neural information processing systems*, 30, 2017.

[71] Yangyang Yu et al. Fincon: A synthesized LLM multi-agent system with conceptual verbal reinforcement for enhanced financial decision making. *Advances in Neural Information Processing Systems*, 37:137010–137045, 2024.

[72] Rui Zhang et al. “Adversarial examples” for proof-of-learning. In *2022 IEEE Symposium on Security and Privacy (SP)*, pages 1408–1422. IEEE, 2022.

[73] Ziqi Zhang et al. No privacy left outside: On the (in-) security of TEE-shielded DNN partition for on-device ML. In *2024 IEEE Symposium on Security and Privacy (SP)*, pages 3327–3345. IEEE, 2024.

[74] Yukun Zhu et al. Aligning books and movies: Towards story-like visual explanations by watching movies and reading books. In *Proceedings of the IEEE international conference on computer vision*, pages 19–27, 2015.

## A Operations and Properties in PAL<sup>\*M</sup>

Table 7 describes supported operations in PAL<sup>\*M</sup> and resulting property attestations.

Table 7: Operations and property attestations in PAL<sup>\*M</sup>

Operation ( <i>op</i> )	Property Attestation
Preprocessing	Proof of preprocessing
Attribute distribution	Proof of attribute distribution
Measurement binding	Proof of binding
Training	Proof of training
Weight optimization	Proof of optimization
Fine-tuning	Proof of fine-tuning
Quantization	Proof of quantization
Evaluation	Proof of evaluation
Inference	Proof of inference
Chat session inference	Proof of session inference